



Long-term performance monitoring of the Adaptive Optics Facility

Pascale Hibon^a, Johann Kolb^b, Philippe Duhoux^b, and Klaas Meinke^c

^aESO Chile, Alonso de Cordova 3107, Santiago, Chile

^bESO Germany, Karl-Schwarzschild-Straße 2, Garching bei München, Germany

^cHadrian Security, Leidseplein 1, Amsterdam, The Netherlands

ABSTRACT

The Adaptive Optics Facility (AOF) started regular operations at the Very Large Telescope (VLT/ESO) in 2016 on the Unit Telescope 4 (UT4). We have now gathered several years of AO telemetry data for the following modules: GALACSI, GRAAL, the 4LGSF and the DSM. I will present here the tool and strategy implemented for monitoring these modules, their performance since 2021, and how this regular monitoring is helping with operations and maintenance activities.

Keywords: AO systems, Performance, Telemetry, Mirror, Lasers, VLT

1. INTRODUCTION

The AOF [2] equips one of the VLT Unit Telescopes at ESO's Paranal Observatory in Chile. It is composed of a Deformable Secondary Mirror (DSM, [1]), four Sodium Lasers to generate artificial Guide Stars (4LGSF, [5]), two Wavefront Sensor modules (GRAAL, [6] and GALACSI, [9]), Real-Time Computers (SPARTA) and other auxiliary equipment. This facility is currently feeding the MUSE [3], HAWK-I [7] and ERIS [4] instruments with AO-corrected Wavefronts and has been available to the Science community for several years. In the future, it will also feed the new instrument MAVIS [8].

Performance monitoring involves the measurement of performance over time against indicators of performance or key performance indicators (KPIs). The two main motivations are to oversee the general health of the VLT systems (telescopes, AO modules, instruments, etc..) as well as to improve the quality of the data products and to optimize the scheduling of technical activities (maintenance, performance optimization, etc..). It is also useful to conduct real-time monitoring of the system status and detailed recordings of the operational data of such a system to improve its overall performance.

Further author information: (Send correspondence to P. Hibon: E-mail: phibon@eso.org, Telephone: 56 2 2463 3084

2. DATA & METHOD

2.1 DATA

The Health Check Monitor provides quick feedback on the performance of the VLT/VLTI instruments. The tool monitors the most relevant instrument and system components, defined by the expert team. The Health Check process is fed by calibrations taken regularly. For GALACSI and GRAAL, the Health Check templates are configured to run every day at the end of the Science Calibrations, with each step at different frequencies (daily, weekly...).

In the case of the AOF, technical templates are executed during the day and the night to record data informing on the Health and Performance of the AO systems. The templates do not process any data, just collect and save it to the disk in a folder with a timestamp. The data can be image cubes, SPARTA loop data (intensities, DM commands...), text files, configuration files (list of actuators)... The processing of this raw data has been recently automated by K. Meinke during his internship in 2021.

2.2 METHOD

The Paranal DataLab is designed to be used by all level of user expertise, from those who just need to see a report or a predefined dashboard, to very advanced user who needs to build complex data analysis workflows. The Paranal DataLab is composed of different data analysis tools, and engineering datasets collected from the telescopes and their instruments during its operations. The DataLab provides access to this operational and engineering data through the following available tools: Automatic Reports, Kibana (logs and metrics search), Grafana (tool to visualize and study your data in an easy and quick way), and Jupyter notebooks. Healthcheck templates are scheduled to run on the GALACSI and GRAAL instruments. These produce files that are then saved to the datalake. From the datalake, they are processed by the Jupyter notebooks. These are also run on a scheduled basis. The notebooks produce two types of outputs: a PDF document with images and computed parameters as well as Elasticsearch documents, which are then displayed on the Grafana Dashboards. This structure is visualized in Figure 1.

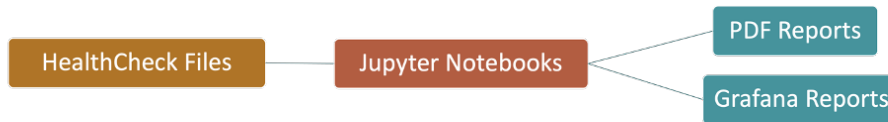


Figure 1. Datalab diagram explaining the dataflow between the different data analysis tools it contains.

3. RESULTS

For all the following figures, red horizontal solid lines represent the threshold values. The vertical dashed lines are showing the following: green: the system is OK, grey: an alert has been triggered for No Data, red: an alert has been triggered for abnormal value.

3.1 DSM

Several parameters are monitored as shown in the following figures. Figure. 2 presents the DSM positions (left panel) and tip-tilt (right panel) to identify any possible anormal forces. Figure. 3 contains three panels allowing us to compare conditions such as temperatures and humidity of the different DSM and its subsystems with the ambient conditions, outside and inside the enclosure. These plots provide valuable information especially in the preparation for future intervention but also in terms of operations: after possible long periods of high humidity, bad weather, and closed dome.

Figure. 4 reports how the DSM actuators state (fully enable, in open-loop, fully disabled) is accounted for in

GRAAL and GALACSI. Indeed if a DSM actuator state is changed, new AO matrices need to be calculated and archived to ensure they are actualized with the correct DSM configuration.

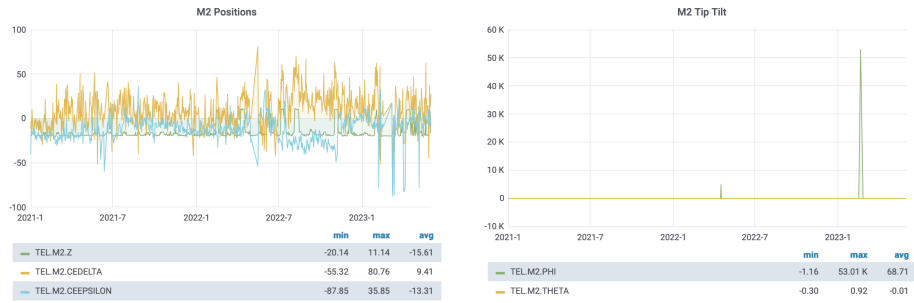


Figure 2. DSM positions and Tip-Tilt to identify any abnormal forces.

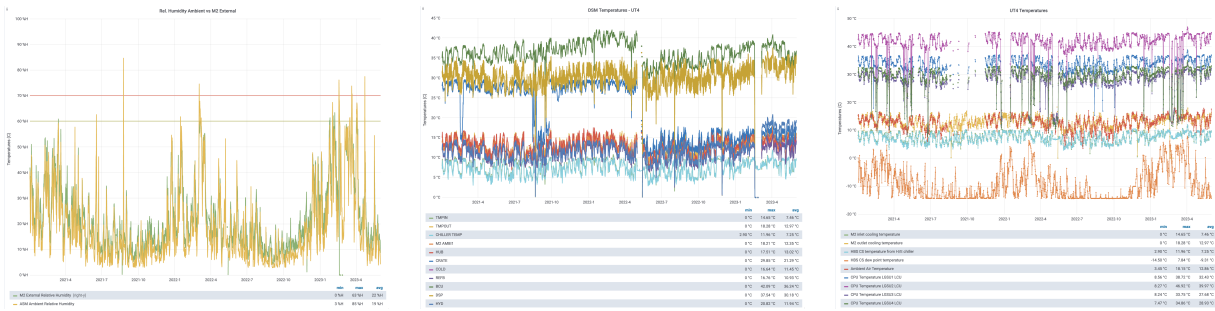


Figure 3. Comparison between the ambient conditions and DSM subsystems sensors.

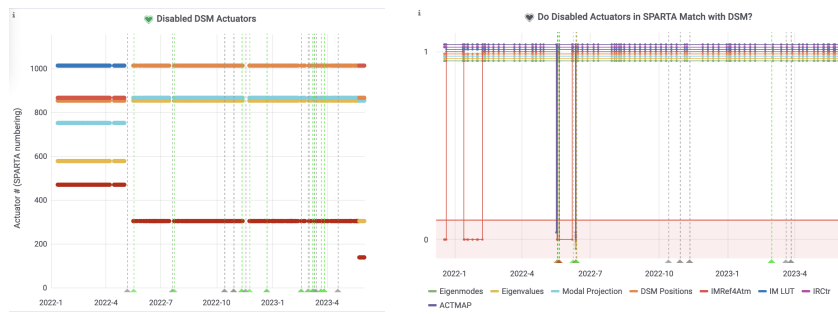


Figure 4. Checks that the DSM actuators state is correctly accounted in GRAAL and GALACSI.

3.2 4LGSF

A complete Dashboard to report on the 4LGSF health and usage has been developed monitoring their power, start-up duration, propagation time, and number of propagations in total and per night. Technical dashboards are also available to monitor its cooling system, central processing unit (CPU), wavelength and power, stability, etc.. In the following figures, we are presenting the statistics for each individual LGSF on their accumulated uptime (Fig. 5), propagation time (Fig. 6), number of propagations (Fig. 7), their percentage (Fig. 8) and their average (Fig. 9) of their propagation time versus their uptime. This is important information in terms of operations to ensure the 4LGSF have a consistent lifetime expectation and usage, especially now that ERIS is in operations using only one LGSF at a time.

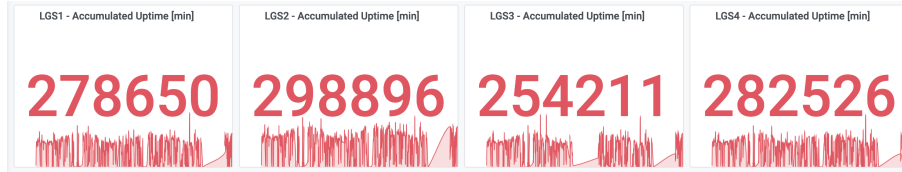


Figure 5. 4LGSF Accumulated Uptime (min).

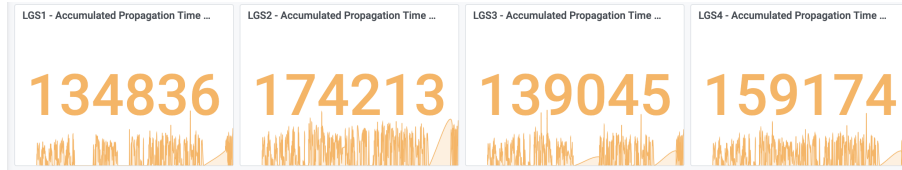


Figure 6. 4LGSF Accumulated Propagation Time (min).

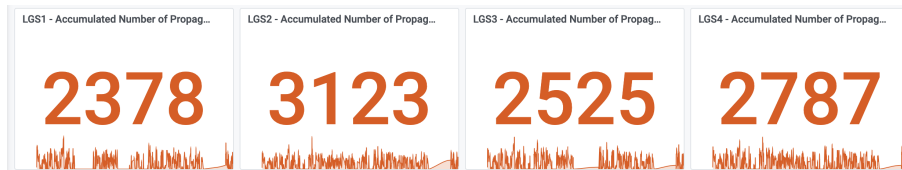


Figure 7. 4LGSF Accumulated Number of Propagations.

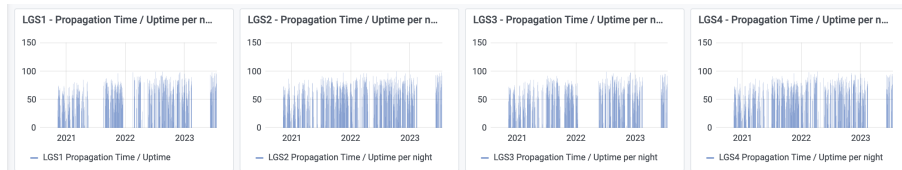


Figure 8. 4LGSF Propagation time / Uptime Percentage.

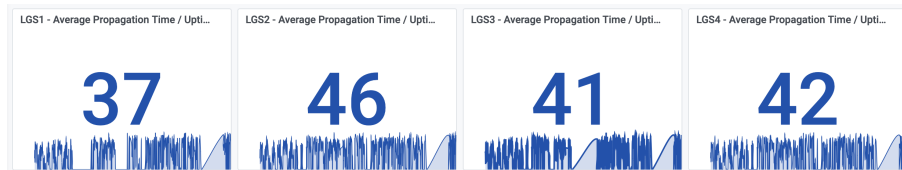


Figure 9. 4LGSF Propagation time / Uptime Average.

3.3 GALACSI

There are several parameters to be monitored for such a complex AO module that is GALACSI, but also for its SPARTA RTC. The exhaustive list is not included here. In the following figures, we are only presenting a few examples.

The LGS and Visible camera dark outlier pixels are also automatically monitored (Fig. 10) to ensure their number does not increase. The most advanced dashboards display both night-time data and their variation with another parameter (telescope elevation), and from them build statistics and propose a pointing model update, as shown in the panels of the Figures 11, 12. In the left panels, the proposed new misregistration model is compared to the current one being used. In the middle panel, the new, proposed model is compared to the current 4LGSF pointing model used by GALACSI for the WFM and the NFM, respectively. Finally, in the right panels, we compare the number of sub-apertures valid in SPARTA with the ones in the Control Matrix Look-up Tables of each LGSF, attributing a value of one when they match.

For NFM operations, it is also important to monitor the IRLOS camera image quality by calculating the elliptical

Moffat FWHM (Fig. 13, left panel) and the elongation (Fig. 13, right panel) and checking the number of outliers in the readout noise.

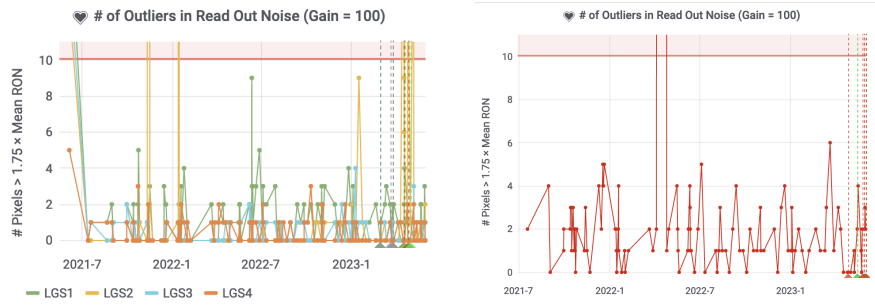


Figure 10. Cameras Darks Outlier pixels: LGS Camera (left), Visible Camera (right).

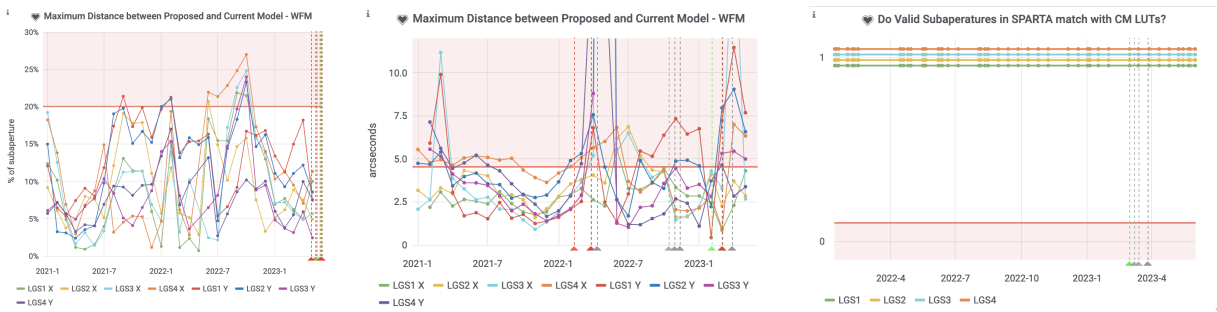


Figure 11. WFM : Left: Comparison of the new, proposed model to the current misregistration model used by GALACSI . Middle: Comparison of the new, proposed model to the current 4LGSF pointing model used by GALACSI. Right: Comparison of the number of valid subapertures in GALACSI to the ones in the control matrix.

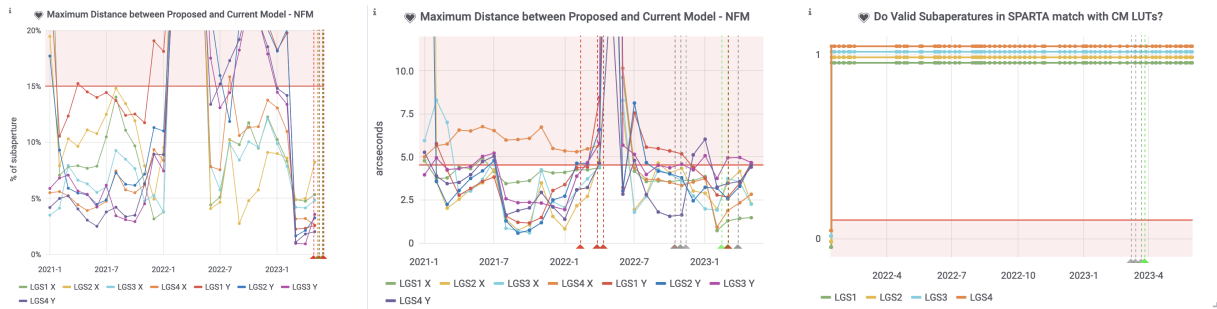


Figure 12. NFM : Left: Comparison of the new, proposed model to the current misregistration model used by GALACSI . Middle: Comparison of the new, proposed model to the current 4LGSF pointing model used by GALACSI. Right: Comparison of the number of valid sub-apertures in GALACSI to the ones in the control matrix.

3.4 GRAAL

In the following figures, we are only presenting a few examples for GRAAL. As GALACSI, the LGS WFSs darks outlier pixels are also automatically monitored (Fig. 14) to ensure their number does not increase, and a spot analysis is performed on the GRAAL LGS WFSs images measuring their FWHM and mean spot elongation (Fig. 15).

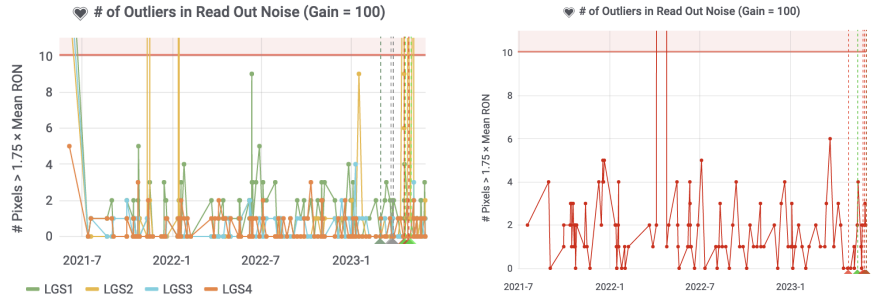


Figure 13. IRLOS Camera Images on MUSE Spot Fitting: Elliptical Moffat FWHM(top) Elongation(bottom).

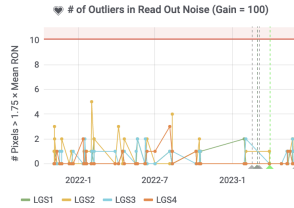


Figure 14. LGS WFS Darks Outlier pixels.

4. DISCUSSION & CONCLUSION

Figure 16 shows the number of DSM actuators in "Open-Loop". We can clearly identify the impact of two major interventions on the DSM. Before May 2022, the DSM was suffering from a cluster of 16 bad actuators. An intervention was then planned and resulted in the recovery of most of them as clearly visible in this figure. Then in February 2023, a major emergency intervention was conducted after the DSM had a major failure. Several actuators had to be set in open loop and a future intervention is now being discussed to recover them, amongst other activities. The change in the quantity of open-loop actuators is again evident in this figure. Such monitoring gives then clear indications of the operational state of such an important AO system and allows us to check that their current state is correctly accounted for in GALACSI and GRAAL.

Figure 17 presents another great example of how useful and helpful performance monitoring can be used to detect and identify technical issues. The top panel monitoring the IRLOS Camera Reference position shows clearly the effect of the Filter Wheel intervention from October 2021 and the quality of the re-calibration of the IRLOS reference position afterwards. In the bottom panel, we can quickly identify when the IRLOS images noise issue was resolved and how stable it remains afterwards.

In conclusion, health checks and performance monitoring for every AOF system have been implemented, although a short non-exhaustive list of examples has been included here.

We confirm the great and valuable method to identify issues, monitor the trend of the main scientific and technical parameters, schedule maintenance and optimize each AOF system performance.

In the future, we plan to develop a complete End-to-End performance monitoring, from the atmosphere photons to the science image quality. This will be first developed for the MUSE Facility. The same strategy should also be prepared and implemented for the new upcoming instruments, defining as early as possible the key parameters to optimize not only the scientific but also the engineering and maintenance operations.

References

- [1] R. Arsenault et al. "A deformable secondary mirror for the VLT". In: *Society of Photo-Optical Instrumentation Engineers (SPIE) Conference Series*. Ed. by Brent L. Ellerbroek and Domenico Bonaccini Calia. Vol. 6272. Society of Photo-Optical Instrumentation Engineers (SPIE) Conference Series. June 2006, 62720V, p. 62720V. DOI: [10.1117/12.672879](https://doi.org/10.1117/12.672879).

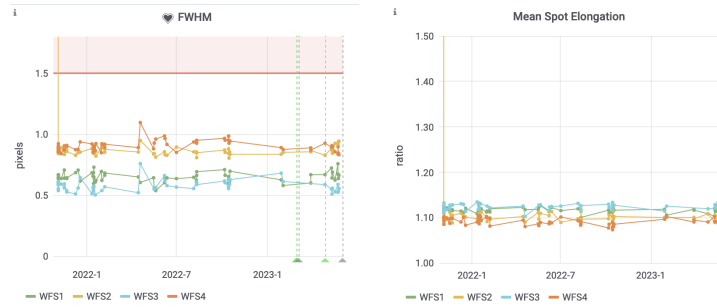


Figure 15. Spot analysis of the GRAAL LGS WFS images.

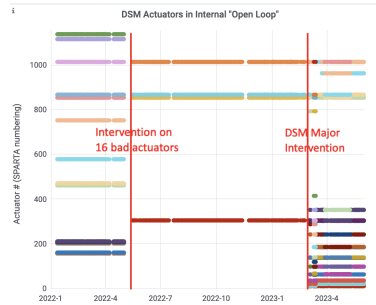


Figure 16. Number of DSM actuators in "Open-Loop".

- [2] R. Arsenault et al. "ESO adaptive optics facility". In: *Adaptive Optics Systems*. Ed. by Norbert Hubin, Claire E. Max, and Peter L. Wizinowich. Vol. 7015. Society of Photo-Optical Instrumentation Engineers (SPIE) Conference Series. July 2008, p. 701524.
- [3] R. Bacon et al. "The MUSE second-generation VLT instrument". In: *Ground-based and Airborne Instrumentation for Astronomy III*. Ed. by Ian S. McLean, Suzanne K. Ramsay, and Hideki Takami. Vol. 7735. Society of Photo-Optical Instrumentation Engineers (SPIE) Conference Series. July 2010, 773508, p. 773508. DOI: [10.1117/12.856027](https://doi.org/10.1117/12.856027). arXiv: [2211.16795](https://arxiv.org/abs/2211.16795) [astro-ph.IM].
- [4] R. Davies et al. "ERIS: revitalising an adaptive optics instrument for the VLT". In: *Ground-based and Airborne Instrumentation for Astronomy VII*. Ed. by Christopher J. Evans, Luc Simard, and Hideki Takami. Vol. 10702. Society of Photo-Optical Instrumentation Engineers (SPIE) Conference Series. July 2018, 1070209, p. 1070209. DOI: [10.1117/12.2311480](https://doi.org/10.1117/12.2311480). arXiv: [1807.05089](https://arxiv.org/abs/1807.05089) [astro-ph.IM].
- [5] W. Hackenberg et al. "Assembly and test results of the AOF laser guide star units at ESO". In: *Adaptive Optics Systems IV*. Ed. by Enrico Marchetti, Laird M. Close, and Jean-Pierre Vran. Vol. 9148. Society of Photo-Optical Instrumentation Engineers (SPIE) Conference Series. Aug. 2014, 91483O, 91483O. DOI: [10.1117/12.2057167](https://doi.org/10.1117/12.2057167).
- [6] Jérôme Paufigue et al. "GRAAL on the mountaintop". In: *Adaptive Optics Systems V*. Ed. by Enrico Marchetti, Laird M. Close, and Jean-Pierre Vran. Vol. 9909. Society of Photo-Optical Instrumentation Engineers (SPIE) Conference Series. July 2016, 99092H, 99092H. DOI: [10.1117/12.2232826](https://doi.org/10.1117/12.2232826).
- [7] Jean-Francois Pirard et al. "HAWK-I: A new wide-field 1- to 2.5- μm imager for the VLT". In: *Ground-based Instrumentation for Astronomy*. Ed. by Alan F. M. Moorwood and Masanori Iye. Vol. 5492. Society of Photo-Optical Instrumentation Engineers (SPIE) Conference Series. Sept. 2004, pp. 1763–1772. DOI: [10.1117/12.578293](https://doi.org/10.1117/12.578293).
- [8] François Rigaut et al. "MAVIS conceptual design". In: *Society of Photo-Optical Instrumentation Engineers (SPIE) Conference Series*. Vol. 11447. Society of Photo-Optical Instrumentation Engineers (SPIE) Conference Series. Dec. 2020, 114471R, 114471R. DOI: [10.1117/12.2561886](https://doi.org/10.1117/12.2561886).

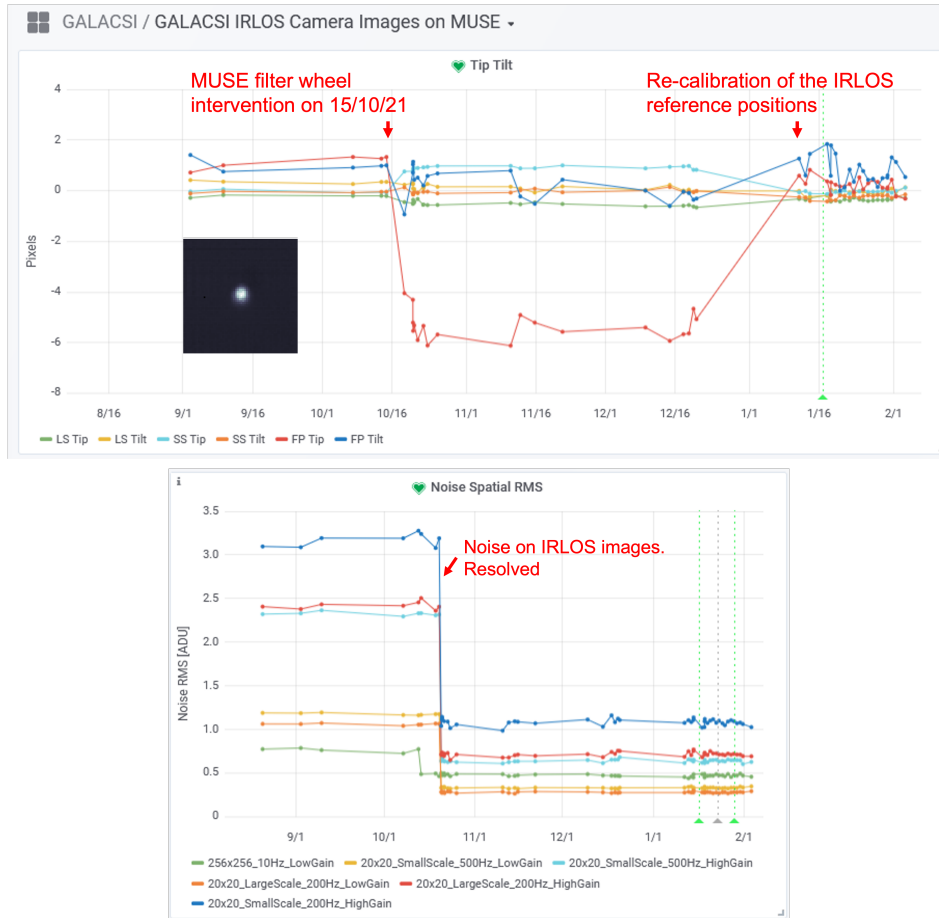


Figure 17. Top: IRLOS Camera Reference position. Bottom: IRLOS Noise spatial RMS.

- [9] S. Ströbele et al. "GALACSI system design and analysis". In: *Adaptive Optics Systems III*. Ed. by Brent L. Ellerbroek, Enrico Marchetti, and Jean-Pierre Véran. Vol. 8447. Society of Photo-Optical Instrumentation Engineers (SPIE) Conference Series. July 2012, 844737, p. 844737. DOI: [10.1117/12.926110](https://doi.org/10.1117/12.926110).